

Spin reorientation transition in the incommensurate stripe-ordered phase of $\text{La}_{3/2}\text{Sr}_{1/2}\text{NiO}_4$

P. G. Freeman,* A. T. Boothroyd, and D. Prabhakaran
Department of Physics, Oxford University, Oxford, OX1 3PU, United Kingdom

D. González
Instituto de Ciencia de Materials de Aragón, CSIC-Universidad de Zaragoza, 50009 Zaragoza, Spain

M. Enderle
Institut Laue-Langevin, BP 156, 38042 Grenoble Cedex 9, France
 (Dated: October 26, 2018)

The spin ordering of $\text{La}_{3/2}\text{Sr}_{1/2}\text{NiO}_4$ was investigated by magnetization measurements, and by unpolarized- and polarized-neutron diffraction. Spin ordering with an incommensurability $\varepsilon \approx 0.445$ is observed below $T_{\text{SO}} \sim 80$ K. On cooling, a spin reorientation is observed at 57 ± 1 K, with the spin axes rotating from $52 \pm 4^\circ$ to $78 \pm 3^\circ$. This is the first time a spin reorientation has been observed in a $\text{La}_{2-x}\text{Sr}_x\text{NiO}_{4+\delta}$ compound having incommensurate stripe order.

Incommensurate magnetic fluctuations observed in superconducting $\text{La}_{2-x}\text{Sr}_x\text{CuO}_4$ (LSCO)¹ are widely believed to be associated with charge stripe correlations.² Assuming this to be the case, it has been concluded that charge stripes in LSCO lie parallel to the Cu–O bonds in the CuO planes for $x \geq 0.053$,³ but are aligned at 45° to the Cu–O bond for $x \leq 0.07$.^{3,4} Given that the critical doping level for superconductivity in LSCO is $x = 0.053$ – 0.056 ,³ these observations suggest a strong link between spin-charge stripe ordering and high temperature superconductivity.

Diagonal charge stripes have also been observed in $\text{La}_{2-x}\text{Sr}_x\text{NiO}_{4+\delta}$ (LSNO),⁵ and have been studied by neutron^{6,7,8,9,10} and x-ray^{11,12} diffraction for doping levels in the range $0.135 \leq x \leq 0.5$. The charge stripes are found to be ordered over a long range, with correlation lengths in excess of 100 \AA for certain levels of doping^{7,12}. LSNO with $x = 1/3$ has stripe order that is particularly stable owing to a commensurability effect that pins the charges to the lattice.^{7,9,13} Having charge stripes that are static and well correlated, LSNO is a good system for studying the basic properties of spin-charge stripes.

Recently, Lee *et al.*⁸ measured the direction of the ordered Ni moments in the spin-ordered phase of compounds with $x = 0.275$ and $1/3$. The angle between the spin axes and the stripe direction was found to be larger at $x = 1/3$ than $x = 0.275$. Furthermore, a transition was observed at ~ 50 K in the $x = 1/3$ sample such that on cooling the spins rotate away from the stripe direction and a further localization of the charge ordering occurs. Lee *et al.* concluded from this that an intimate connection exists between the local spin order and the stability of the charge order.

Early work on $\text{La}_{3/2}\text{Sr}_{1/2}\text{NiO}_{4+\delta}$ by electron diffraction¹⁴ suggested that the case of half-doping is another very stable charge-ordering phase. This charge ordering has a 2-D checkerboard-like pattern as shown in figure 1(a). Recently, Kajimoto *et al.*¹⁰ studied the spin and charge order in a single crystal of

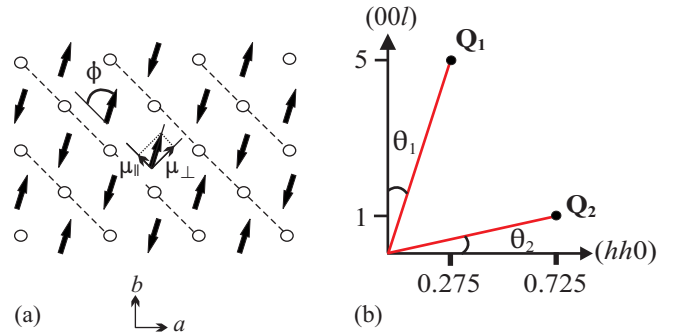


FIG. 1: (a) Ideal checkerboard 2-D charge ordering in the ab plane. Circles represent holes residing on Ni sites, while the solid arrows represent the spins of the Ni^{2+} sites. Dashed lines indicate the charge domain walls common to both checkerboard and stripe ordering. The commensurate spin ordering shown here is not realized in practice in $\text{La}_{3/2}\text{Sr}_{1/2}\text{NiO}_{4+\delta}$. The observed spin order in $\text{La}_{3/2}\text{Sr}_{1/2}\text{NiO}_{4+\delta}$ is similar to that shown, but is actually incommensurate in the direction perpendicular to the stripes. The components of the ordered moment parallel (μ_{\parallel}) and perpendicular (μ_{\perp}) to the stripe direction are shown, and ϕ denotes the angle between the spin axis and the stripe direction. (b) Diagram of the (h, h, l) plane in reciprocal space. \mathbf{Q}_1 and \mathbf{Q}_2 are the scattering vectors of the two magnetic peaks investigated in this work.

$\text{La}_{3/2}\text{Sr}_{1/2}\text{NiO}_4$ by neutron diffraction. They observed checkerboard ordering below ~ 480 K, but they also found an incommensurate charge-stripe ordering phase below $T_{\text{ICO}} \sim 180$ K coexisting with the checkerboard ordering. Spin ordering was reported to be found only in association with the incommensurate component of the charge ordering.

Here we describe a study of spin-ordering in $\text{La}_{3/2}\text{Sr}_{1/2}\text{NiO}_{4+\delta}$ employing magnetometry and polarized- and unpolarized-neutron diffraction. Our results are consistent with those of Kajimoto *et al.*,¹⁰ but in addition we observed a spin reorientation

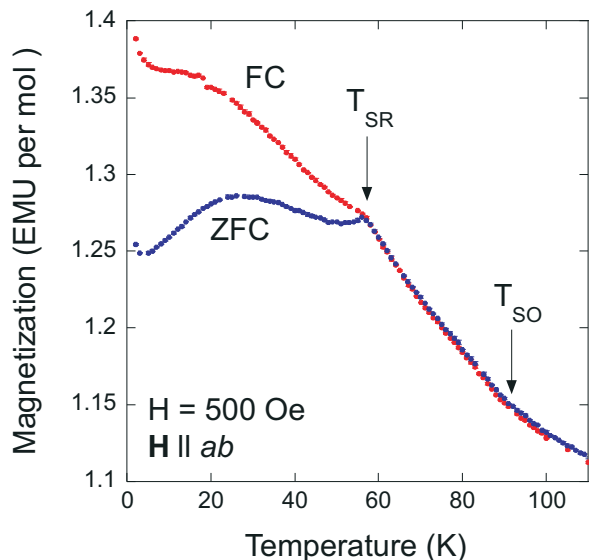


FIG. 2: FC and ZFC magnetization data for $\text{La}_{3/2}\text{Sr}_{1/2}\text{NiO}_{4+\delta}$. Arrows indicate the spin-ordering temperature, T_{SO} , and the spin-reorientation temperature, T_{SR} .

transition similar to, but more pronounced than that observed in $\text{La}_{5/3}\text{Sr}_{1/3}\text{NiO}_4$. This is the first time a spin reorientation associated with an incommensurate spin ordering has been observed in a LSNO material. The spin reorientation is signalled by a sharp anomaly in the magnetization at ~ 57 K, and an analysis of polarized-neutron diffraction data shows that on cooling through 57 K the Ni spins rotate away from the stripe direction.

Two single crystals of $\text{La}_{3/2}\text{Sr}_{1/2}\text{NiO}_{4+\delta}$ were used for these experiments. The crystal used for the magnetization measurements had dimensions $\sim 7 \times 5 \times 2 \text{ mm}^3$ and that for neutron diffraction was a rod of 7–8 mm diameter and ~ 35 mm in length. Both these samples were grown from the same starting powder by the floating-zone technique.¹⁵ The oxygen excess was determined by thermogravimetric analysis to be $\delta = 0.02 \pm 0.01$.

Magnetization data were collected with a SQUID magnetometer (Quantum Design) with the field applied parallel to the ab plane of the crystal. We carried out DC measurements by cooling in an applied field of 500 Oe (FC) and also by cooling in zero field and measuring while warming in a field of 500 Oe (ZFC). Figure 2 shows the temperature variation of the FC and ZFC magnetization. A small change in slope at 90 ± 5 K marks the spin ordering temperature, in agreement with previous observations.⁷ A clearer anomaly is seen at $T_{\text{SR}} = 57$ K, where the FC and ZFC curves sharply separate. Below 5 K both the FC and ZFC curves begin to rise for reasons that are not yet understood, but could be due to a small amount of paramagnetic impurity in the crystal. We measured the FC magnetization parallel to the crystal c direction (not shown) and found no anomaly

around T_{SR} , thus indicating that the transition involves the in-plane components of the spins.

In what follows we describe neutron diffraction studies aimed at identifying the nature of the transition at T_{SR} . Referred to the tetragonal unit cell of LSNO, with unit cell parameters $a \approx 3.8 \text{ \AA}$, $c \approx 12.7 \text{ \AA}$, charge ordering peaks due to structural distortions are located at $(h \pm \varepsilon, k \pm \varepsilon, l)$ positions in reciprocal space. The spin order peaks are located at $(h+1/2 \pm \varepsilon/2, k+1/2 \pm \varepsilon/2, l)$, the strongest being when l is odd.⁸ To a first approximation the relationship between the incommensurability, ε , and the hole concentration, $n_h = x + 2\delta$, is simply $\varepsilon = n_h$. In general, however, competition between apparently different wavevectors for the spin and charge ordering⁹ and the separate issue of oxygen non-stoichiometry^{14,16,17} causes small deviations from the $\varepsilon = n_h$ rule.

The neutron experiments were performed on the triple-axis spectrometer IN20 at the Institut Laue-Langevin. The energies of the incident and elastically-scattered neutrons were selected by Bragg reflection from an array of either pyrolytic graphite (PG) or Heusler alloy crystals, for unpolarized- and polarized-neutron scattering respectively. A PG filter was present after the sample and before the analyzer to suppress higher-order harmonic scattering. Most of the data were obtained with initial and final neutron wavevectors of 2.66 \AA^{-1} , with some further data taken with a neutron wavevector of 3.54 \AA^{-1} . We mounted the sample with the [001] and [110] crystal directions in the horizontal scattering plane, and performed scans in reciprocal space either parallel to the $(h, h, 0)$ direction at constant l , or parallel to the $(0, 0, l)$ direction at constant h .

We began by performing polarized-neutron diffraction measurements with the neutron polarization \mathbf{P} parallel to the scattering vector \mathbf{Q} , maintained by adjusting currents in a Helmholtz coil mounted around the sample. In this configuration a neutron's spin is flipped during a magnetic scattering process, but remains unchanged when scattered by a non-magnetic process, e.g. from a distortion of the lattice. Thus, by measuring the spin-flip (SF) and non-spin-flip (NSF) channels one can identify whether the origin of the scattering is magnetic or not.

We observed charge-order diffraction in the vicinity of the $(1.5, 1.5, l)$ line in reciprocal space. At $T = 10$ K the peak shape observed in $(h, h, 0)$ scans was consistent with that observed by Kajimoto *et al.*, with a central peak at $h = 1.5$ and two satellites at $h \approx 1.45$ and 1.55 . We observed no variation of this scattering with l over a single Brillouin zone, showing that both the commensurate and incommensurate components of charge ordering are completely two-dimensional.

We observed spin-order diffraction peaks at $(h+1/2 \pm \varepsilon/2, h+1/2 \pm \varepsilon/2, l)$ positions with l odd and $\varepsilon = 0.445 \pm 0.005$. Figure 3 shows a scan parallel to $(0, 0, l)$. The widths of the peaks in this scan convert to a correlation length along the c axis of $16.4 \pm 0.3 \text{ \AA}$. For comparison, the in-plane correlation length in the

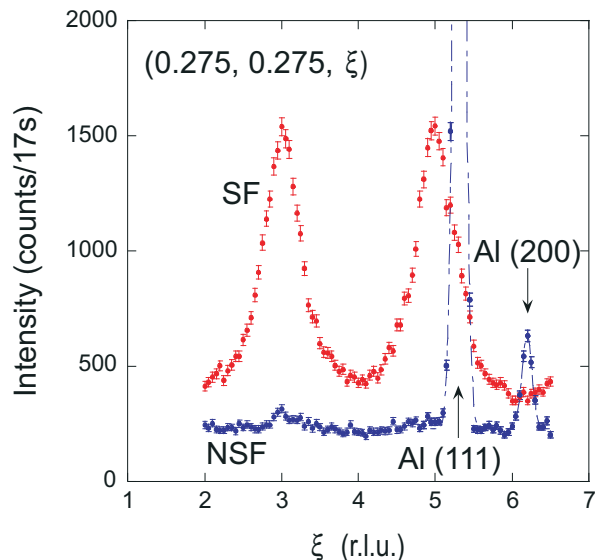


FIG. 3: Spin-flip (SF) and non-spin-flip (NSF) diffraction from $\text{La}_{3/2}\text{Sr}_{1/2}\text{NiO}_4$ at $T = 10$ K. The scan is parallel to $(0, 0, l)$ and passes through the magnetic order peak $(0.275, 0.275, 1)$. No correction has been made for the imperfect polarization of the neutron beam. The sharp peaks in the NSF channel at $l \approx 5.3$ and 6.2 are due to diffraction from the Al sample mount.

direction perpendicular to the stripes is $78.3 \pm 1.3 \text{ \AA}$. There were no peaks at $l = \text{even}$ positions, as can be seen in figure 3. There were also no spin-order peaks at $(h \pm 1/4, h \pm 1/4, 1)$ positions, confirming the lack of any commensurate Fourier component in the spin ordering, in agreement with the observations of Kajimoto *et al.*¹⁰

Figure 4a show the temperature dependence of the integrated intensity of two magnetic reflections, $\mathbf{Q}_1 = (0.275, 0.275, 5)$ and $\mathbf{Q}_2 = (0.275, 0.275, 1)$, measured in scans parallel to $(h, h, 0)$. The spin ordering transition is seen to be rather sluggish, but a sharpening of the peaks below $T_{\text{SO}} \approx 80$ K (not shown) suggests that this is where long-range ordering extending over many unit cells sets in. However short-range correlations persist above 100 K. On cooling below T_{SO} , the peak at \mathbf{Q}_1 increases monotonically, while that at \mathbf{Q}_2 first increases, then reaches a maximum at ~ 60 K, then decreases again. This anomalous behaviour correlates with the transition observed in the magnetization, Fig. 2. To understand this behaviour we must recall that magnetic neutron diffraction is sensitive to spin components perpendicular to \mathbf{Q} . As shown in figure 1(b), \mathbf{Q}_1 is approximately parallel to $(0, 0, l)$ while \mathbf{Q}_2 is approximately parallel to $(h, h, 0)$. Therefore, to a good approximation, the scattering at \mathbf{Q}_1 is from the total in-plane spin moment, irrespective of its direction, while that at \mathbf{Q}_2 comes mainly from the spin components parallel to the stripes and along the c axis. The data in fig. 4a therefore imply that below ~ 57 K the spins rotate away from the stripe direction.

To fully analyze the direction of the spins over this

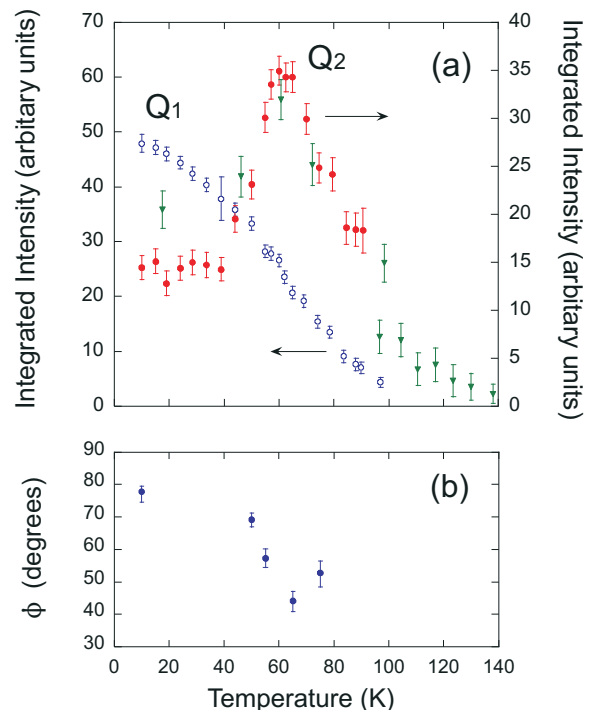


FIG. 4: (a) The peak intensities of the spin peaks $\mathbf{Q}_1 = (0.275, 0.275, 5)$ and $\mathbf{Q}_2 = (0.275, 0.275, 1)$ — see figure 1(b). Circle symbols represent data taken with a neutron wavevector of 3.54 \AA^{-1} and triangles represent 2.66 \AA^{-1} . Filled symbols are data taken at \mathbf{Q}_2 and unfilled symbols at \mathbf{Q}_1 , with the arrows indicating the relevant scales for each \mathbf{Q} . (b) The temperature dependence of the angle ϕ between the spin axis and the stripe direction obtained from polarized-neutron analysis.

temperature range we varied the direction of the neutron polarization \mathbf{P} relative to the scattering vector \mathbf{Q} . Three configuration were used: 1) $\mathbf{P} \parallel \mathbf{Q}$, 2) $\mathbf{P} \perp \mathbf{Q}$ but in the scattering plane, and 3) $\mathbf{P} \perp \mathbf{Q}$ but out of the scattering plane. (Recall that $[110]$ and $[001]$ are the crystal directions in the scattering plane.) As mentioned before, neutrons scatter via magnetic interactions from spin components perpendicular to \mathbf{Q} , and SF scattering is due to spin components perpendicular to \mathbf{P} . Therefore, analysis of configurations 1), 2) and 3) leads to the direction of the ordered moment.¹⁸ Table 1 summarizes the relations between the observed intensities at \mathbf{Q}_1 and \mathbf{Q}_2 and the ordered spin components parallel (μ_{\parallel}) and perpendicular (μ_{\perp}) to the stripe direction (see figure 1(a)), and parallel to the c axis (μ_c).

We corrected the data to take into account the different background count rates in the SF and the NSF channels, and to correct for the imperfect spin polarization of neutron beam. The latter was calculated from the flipping ratio 18.5 ± 1.8 measured on a magnetic Bragg peak.

A full analysis of the intensities at the \mathbf{Q}_1 and \mathbf{Q}_2 points determined the spin orientations at $T = 10$ K and $T = 65$ K. These analyses showed that the non-magnetic (NM) and μ_c count rates were zero, to within error for

P configuration			\mathbf{Q}_1	\mathbf{Q}_2
1)	$\mathbf{P} \parallel \mathbf{Q}$	SF	$\mu_{\perp}^2 \cos^2\theta_1 + \mu_{\parallel}^2 + \mu_C^2 \sin^2\theta_1$	$\mu_{\perp}^2 \sin^2\theta_2 + \mu_{\parallel}^2 + \mu_C^2 \cos^2\theta_2$
		NSF	NM	NM
2)	$\mathbf{P} \perp \mathbf{Q}$ (\mathbf{P} in horiz. plane)	SF	μ_{\parallel}^2	μ_{\parallel}^2
		NSF	$\mu_{\perp}^2 \cos^2\theta_1 + \mu_C^2 \sin^2\theta_1 + \text{NM}$	$\mu_{\perp}^2 \sin^2\theta_2 + \mu_C^2 \cos^2\theta_2 + \text{NM}$
3)	$\mathbf{P} \perp \mathbf{Q}$ (\mathbf{P} vertical)	SF	$\mu_{\perp}^2 \cos^2\theta_1 + \mu_C^2 \sin^2\theta_1$	$\mu_{\perp}^2 \sin^2\theta_2 + \mu_C^2 \cos^2\theta_1$
		NSF	$\mu_{\parallel}^2 + \text{NM}$	$\mu_{\parallel}^2 + \text{NM}$

TABLE I: Expressions for the intensity of SF and NSF scattering for different orientations of the neutron polarization \mathbf{P} relative to the scattering vector \mathbf{Q} (NM is the non-magnetic scattering).

both temperatures. Thus, it is reasonable to assume that the spins lie within the ab plane over the whole temperature range, consistent with the lack of any anomaly observed at T_{SR} in the magnetization data measured with $\mathbf{H} \parallel c$. At the other temperatures we deduced the spin orientation within the ab plane from one \mathbf{Q} position ($T = 55$ K from \mathbf{Q}_1 , $T = 50$ and 75 K from \mathbf{Q}_2 .) From these data we find that the spins reorientate from an angle of $52 \pm 4^\circ$ to the stripe direction at $T = 75$ K, to $78 \pm 3^\circ$ at $T = 10$ K, as shown in figure 4(b). The transition is seen to occur quite rapidly between 50 and 65 K, although the reorientation is not complete at 50 K.

How does the spin reorientation described here in the $x = 1/2$ crystal compare with that reported by Lee *et al.*⁸ for $x = 1/3$? In both compositions the spin reorientations occur at similar temperatures (~ 50 K for $x = 1/3$, ~ 57 K for $x = 1/2$) and the spins rotate in the same sense, namely away from the stripe direction, on cooling. On the other hand, the angle through which the spins rotate is greater for $x = 1/2$ ($\sim 26^\circ$) than for $x = 1/3$ ($\sim 13^\circ$), and the final low temperature spin direction in $x = 1/2$ is almost perpendicular to the stripes ($\phi = 78^\circ$) compared with 53° for $x = 1/3$. Considering also the spin direction $\phi = 27^\circ$ observed for $x = 0.275$,⁸ for which there is no reorientation transition, we find that as the doping level increases the angle from the stripe

direction increases. However, the trend in the spin orientation also correlates with the increasing stability of the charge ordering as measured by the charge-ordering temperatures^{7,8,10} ($T_{\text{CO}}(x = 0.275) \sim 200$ K, $T_{\text{CO}}(x = 1/3) \sim 240$ K, $T_{\text{CO}}(x = 1/2) \sim 480$ K). Therefore, measurements on more compositions of $\text{La}_{2-x}\text{Sr}_x\text{NiO}_{4+\delta}$ are needed to establish whether it is the doping level or the stability of the charge order that is more important in determining the spin orientation.

The occurrence of spin reorientation transitions in the $x = 1/3$ and $x = 1/2$ but not in $x = 0.275$ might suggest that these transitions are linked to the stability of the charge order. Irrespective of this, what the present study has shown is that the occurrence of a spin reorientation transition does not depend on the stripe order being commensurate with lattice. Indeed, the spin reorientation transition is even more striking in the $x = 1/2$ composition, for which the spin order is incommensurate, than in $x = 1/3$, for which it is commensurate.

These observations emphasize the importance of couplings between spin and charge degrees of freedom in stripe-ordered systems, and suggest that this coupling is particularly strong in $\text{La}_{3/2}\text{Sr}_{1/2}\text{NiO}_4$.

This work was supported in part by the Engineering and Physical Sciences Research Council of Great Britain.

* URL: <http://xray.physics.ox.ac.uk/Boothroyd>

¹ T. R. Thurston *et al.*, Phys. Rev. B **40**, 4585 (1989); S-W. Cheong *et al.*, Phys. Rev. Lett. **67**, 1791 (1991); T. E. Mason, G. Aeppli, and H. A. Mook, Phys. Rev. Lett. **68**, 1414 (1992); T. R. Thurston *et al.*, Phys. Rev. B **46**, 9128 (1992);
² J. M. Tranquada *et al.*, Nature (London) **375**, 561 (1995).
³ M. Fujita *et al.*, Phys. Rev. B **65**, 064505 (2002).
⁴ S. Wakimoto *et al.*, Phys. Rev. B **60**, R769 (1999); S. Wakimoto *et al.*, Phys. Rev. B **61**, 3699 (2000); M. Matsuda *et al.*, Phys. Rev. B **62**, 9148 (2000).
⁵ J. M. Tranquada, D. J. Buttrey, D. E. Rice, Phys. Rev. Lett. **70**, 445 (1993)
⁶ S. M. Hayden *et al.*, Phys. Rev. Lett. **68**, 1061 (1992); V. Sachan *et al.*, Phys. Rev. B **51**, 12742 (1995); J. M. Tranquada, D. J. Buttrey, and V. Sachan, Phys. Rev. B **54**, 12318 (1996);

⁷ H. Yoshizawa *et al.*, Phys. Rev. B **61**, R854 (2000)

⁸ S-H. Lee *et al.*, Phys. Rev. B **63**, 060405 (2001)

⁹ R. Kajimoto *et al.*, Phys. Rev. B **64**, 144432 (2001)

¹⁰ R. Kajimoto *et al.*, cond-mat/020228 (2002)

¹¹ E. D. Isaacs *et al.*, Phys. Rev. Lett. **72**, 3421 (1994); A. Vigliante *et al.*, Phys. Rev. B **56**, 8248 (1997)

¹² Yu. G. Pashkevich *et al.*, Phys. Rev. Lett. **84**, 3919 (2000)

¹³ A. P. Ramirez *et al.*, Phys. Rev. Lett. **76**, 447 (1996)

¹⁴ C. H. Chen, S-W. Cheong, and A. S. Cooper, Phys. Rev. Lett. **71**, 2461 (1993)

¹⁵ D. Prabhakaran, P. Isla, and A. T. Boothroyd, J. Cryst. Growth **237**, 815 (2002)

¹⁶ Th. Jestädt *et al.*, Phys. Rev. B **59**, 3775 (1999)

¹⁷ P. Wochner *et al.*, Phys. Rev. B **57**, 1066 (1998)

¹⁸ Actually, 2 out of the 3 configurations are sufficient.